Mixed Analog-Digital Implementation of the Semidiscrete Wavelet Transform

Marco A. Gurrola-Navarro and Guillermo Espinosa-Flores-Verdad

National Institute for Astrophysics Optics and Electronics Electronics Department Tonantzintla, Mexico magurrola@inaoep.mx, gespino@inaoep.mx

(Paper received on February 29, 2008, accepted on April 15, 2008)

Abstract. In the present work is proposed a mixed approach to implement the two parts of the wavelet transform: the direct transform using analog filters and the inverse transform by digital filters. A set of continuous time signals, constituting the wavelet transform, is obtained from the original signal using analog filters. This set of signals is digitalized and then the inverse wavelet transform can be numerically applied. The digital filters are specially designed to compensate linear variations on the analog devices as well as the effects of the finite number of scales in the system. The difference between the reconstructed and the original signal can be as low as be required.

1 Introduction

The Wavelet Transform (WT) maps a time signal to a function depending on two variables: time location and scale. The WT allows the representation of a signal simultaneously in time and frequency, and is "particularly useful for analyzing signals which can best be described as aperiodic, noisy, intermittent, transient and so on" [1]. Denoising, compression, pattern recognition and enhancement are some of the techniques specially developed to be applied in the wavelet domain and are used in application areas as image processing, medicine, engineering, physics, etc. [1][2][3].

In the most works about the WT its numerical implementation by software or digital hardware is supposed. Only few works deal with the alternative to carry out the WT using analog circuits. In this work is taken the approach to implement the WT by convolution in continuous time filters [4][5][6][7][8][9]. In particular, the set of continuous band-pass filters defined in [9] is here taken to perform the direct WT, whereas the inverse transform is numerically developed using a wavelet which is constructed as is explained in [10].

The proposal of the analog implementation of the direct WT in combination with a numerical implementation of the inverse WT is an original contribution of this work. Additionally, in this paper is explained how to fit the numerical wavelets to compensate linear deviations on the analog wavelets due to non-ideal devices, and how to design two lateral filters to compensate the effects due to the

© E. V. Cuevas, M. A. Perez, D. Zaldivar, H. Sossa, R. Rojas (Eds.) Special Issue in Electronics and Biomedical Informatics, Computer Science and Informatics
Research in Computing Science 35, 2008, pp. 117-124



finite number of scales in the system. This corrections make possible to obtain an error between the reconstructed and the original signals as low as be required.

Section 2 is a review of the theoretical bases of the semidiscrete WT. The compensation of the variations on the analog wavelets and the effects of the finite number of scales are explained in sections 3 and 4. A simulation example is shown in section 5. And the conclusions are depicted in section 6.

2 Semidiscrete Wavelet Transform

Given a function f(t), in this work the complex conjugated is denoted by $f^*(t)$ and its Fourier transform is denoted by the respective upper case letter, $F(\omega)$, except H(s) representing the Laplace transform of h(t).

2.1 General Principles

The direct and inverse semidiscrete WT of a function f(t) respect to the prototype wavelet $\psi(t)$ are given by [11][10]

$$w_m(b) = \int_{-\infty}^{\infty} f_{in}(t)\psi_m(t-b)dt, \qquad (1)$$

$$f_{out}(t) = \sum_{m} \int_{-\infty}^{\infty} w_m(b) \chi_m(t-b) db, \qquad (2)$$

where $m \in \mathbb{Z}$, and

$$\psi_m(t) = r^{-m}\psi(r^{-m}t), \qquad (3)$$

for a selected value $1 < r \in \mathbb{R}$. As can be seen, the semidiscrete WT is defined by the set of continuous functions $w_m(t)$.

To be used as semidiscrete wavelet, $\psi(t)$ must be bounded and integrable, must fulfill the admissibility condition

$$\int_{-\infty}^{\infty} \frac{|\Psi(\omega)|^2}{\omega} d\omega < \infty, \text{ for } \omega > 0,$$
(4)

and must satisfy the stability condition: there exist two constants A and B, with $0 < A \le B < \infty$, such that for every $\omega > 0$

$$A \le \sum_{m} |\Psi(r^m \omega)|^2 \le B. \tag{5}$$

To achieve perfect reconstruction, for $\omega > 0$ must be verified

$$\sum_{m} \Psi^*(r^m \omega) X(r^m \omega) = 1.$$
 (6)

Analog Wavelet Filters 2.2

Work [9] shows that any continuous linear filter described in the Laplace domain

$$H(s) = \frac{p_1 s + p_2 s^2 + \dots + p_{d-1} s^{d-1}}{q_0 + q_1 s + \dots + q_{d-1} s^{d-1} + s^d},$$
 (7)

where $2 \leq d \in \mathbb{Z}$, $p_1, \dots, p_{d-1}, q_0, \dots, q_{d-1} \in \mathbb{R}$, with at least one p different to zero, and denominator is a strictly Hurwitz polynomial, has an impulse response h(t), such that $\psi(t) = h(-t)$ is a semidiscrete wavelet for any value r > 1, i.e. $\psi(t)$ is bounded, is integrable, and satisfies the admissibility (4) and stability (5)

Therefore, the equation (1) can be implemented in a continuous time filter by the convolution between the input signal $f_{in}(t)$ and the impulse response

Numerical Wavelets

In the work [10] is defined the function

$$X(\omega) = \frac{\Psi(\omega)}{\sum_{m} |\Psi(r^{m}\omega)|^{2}},$$
(8)

which fulfills the condition for perfect reconstruction (6) as can be easy probed by direct substitution.

Having the numerical representation of $\chi(t)$, the inverse WT (2) can be numerically implemented after the analog-to-digital conversion of $w_m(t)$.

Compensation of Linear Variations 3

Suppose that the functions $H_{\psi_m}(j\omega) = \Psi^*(r^m\omega)$ are implemented with analog circuits and that variations in the time constants are introduced due to deviations on the nominal values of the analog devices.

If the deviations introduce only linear changes in the filter responses (without distortion), then the effects can be compensated using the function

$$\bar{\mathbf{X}}_{m}(\omega) = \frac{\Psi^{*}(r^{m}\omega)}{\bar{\Psi}_{m}^{*}(\omega)} \mathbf{X}(r^{m}\omega), \qquad (9)$$

where $\bar{\Psi}_m^*(\omega)$ is the actually implemented analog m filter.

Making direct substitutions can be easily verified that the functions $\bar{\Psi}_m(\omega)$ and $\bar{\mathbf{X}}_m(\omega)$ fulfill condition (6).

4 Compensation of Bandpass Behavior

In practice only systems with a finite number of filters can be implemented. The filters go from the lower scale m_a up to the higher scale m_b . The operative frequency range of the system can be established as $\omega \in (\omega_b, \omega_a)$, where ω_a and ω_b are the central frequencies of the first and last filters, $\Psi_{m_a}(\omega)$ and $\Psi_{m_b}(\omega)$. However the lacking filters of scales lower than m_a and higher than m_b will bring about the unfulfillment of condition (6), introducing a band pass behavior in the finite sum $\sum_{m=m_a}^{m_b} \Psi^*(r^m\omega)X(r^m\omega)$.

This band-pass behavior can be compensated on $\omega \in (\omega_b, \omega_a)$ redefining the next lateral filters which involve n extra scales at each side.

$$\bar{\mathbf{X}}_{m_a}(\omega) = \frac{\sum_{m=m_a-n}^{m_a} \Psi_m^*(\omega) \mathbf{X}_m(\omega)}{\bar{\Psi}_{m_a}^*(\omega)}, \qquad (10)$$

$$\bar{\mathbf{X}}_{m_b}(\omega) = \frac{\sum_{m=m_b}^{m_b+n} \Psi_m^*(\omega) \mathbf{X}_m(\omega)}{\bar{\Psi}_{m_b}^*(\omega)}.$$
 (11)

The functions $\bar{\Psi}_m(\omega), \bar{\bf X}_m(\omega), \bar{\bf X}_{m_a}(\omega)$ and $, \bar{\bf X}_{m_b}(\omega)$ satisfies

$$\bar{\Psi}_{m_a}^*(\omega)\bar{X}_{m_a}(\omega) + \sum_{m=m_a+1}^{m_b-1} \bar{\Psi}_m^*(\omega)\bar{X}_m(\omega) + \bar{\Psi}_{m_b}^*(\omega)\bar{X}_{m_b}(\omega) =
= \sum_{m=m_a-n}^{m_b+n} \Psi^*(r^m\omega)X(r^m\omega) \approx 1, \text{ for } \omega \in (\omega_b, \omega_a).$$
(12)

As larger is n the error of reconstruction will be lower, as can be seen in the example of next section.

5 Simulated Example

For the WT system of this example a value $r=\sqrt[3]{10}$ was selected, obtaining three scales per decade. The prototype filter is given by

$$H_{\psi_0}(s) = \frac{(s\omega_c/q)^2}{(s^2 + s\omega_c/q + \omega_c)^2},$$
 (13)

where $\omega_c = 2\pi \times 10 \,\mathrm{Hz}$ and $q = \sqrt{1/2}$.

The system has 7 filters from $m_a=0$ to $m_a=6$ and operates in the frequency range (0.1 Hz, 10 Hz). Only two extra scales (n=2) were considered at each side to construct the lateral filters.

Table 1 shows the central frequency of the filters $H_{\psi_m}(s)$.

Fig. 1 shows the ideal analog $\psi_0(t)$ and numerical $\chi_0(t)$ wavelets.

Fig. 2-a shows the spectrums of $H_{\psi_m}(j\omega)$, both ideal and with simulated linear variations. The variations was introduced with Gaussian deviations of $20\% = 3\sigma$ in the poles of the transference function. The variations has been overdone for illustrative purposes, even though uniform variations with values as low as 1% can be achieved in actual analog integrated circuits when mismatch

design guidelines are carefully followed. Fig. 2-b shows the spectrums of $\bar{X}_m(\omega)$ for m=1 to m=5. Fig. 2-c shows the spectrums of the lateral filters $\bar{\mathbf{X}}_{m_a}(\omega)$ and $\bar{\mathbf{X}}_{m_b}(\omega)$.

Fig. 3-a shows a probe signal $f_{in}(t)$ which includes a chirp signal and oscillations of 0.1, 1.0 and 10 Hz. Fig. 3-b shows the wavelet transform $w_m(t)$ of the signal $f_{in}(t)$. Fig. 3-c shows the difference between the reconstructed signal $f_{out}(t)$ and the probe signal $f_{in}(t)$ (the reconstructed signal was not included because in the resolution of the graphics the differences respect to the probe signal can not be appreciated).

Table 2 shows the the maximum difference $f_{out}(t) - f_{in}(t)$ as a function of the amount of extra scales (n) that was considered in the construction of the lateral filters.

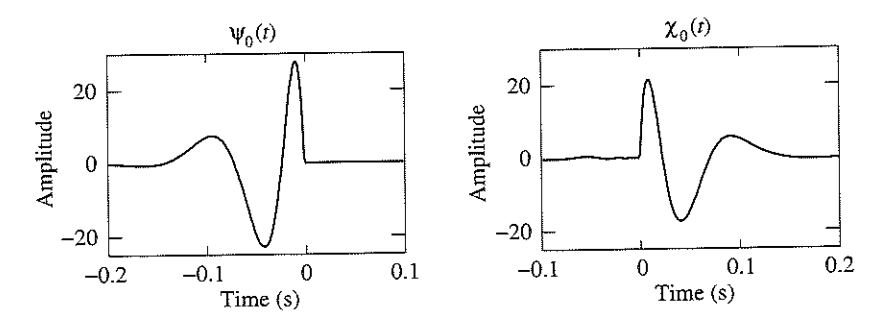


Fig. 1. Analog prototype wavelet $\psi_0(t)$ and numerical wavelet $\chi_0(t)$.

Table 1. Central frequency of the filters $H_{\psi_m}(s)$.

filter (Central Freq.
m	(Hz)
0	$10.0~\mathrm{Hz}$
1	$4.64~\mathrm{Hz}$
2	$2.15~\mathrm{Hz}$
3	$1.00~\mathrm{Hz}$
4	$0.464~\mathrm{Hz}$
5	$0.215~\mathrm{Hz}$
6	0.100 Hz

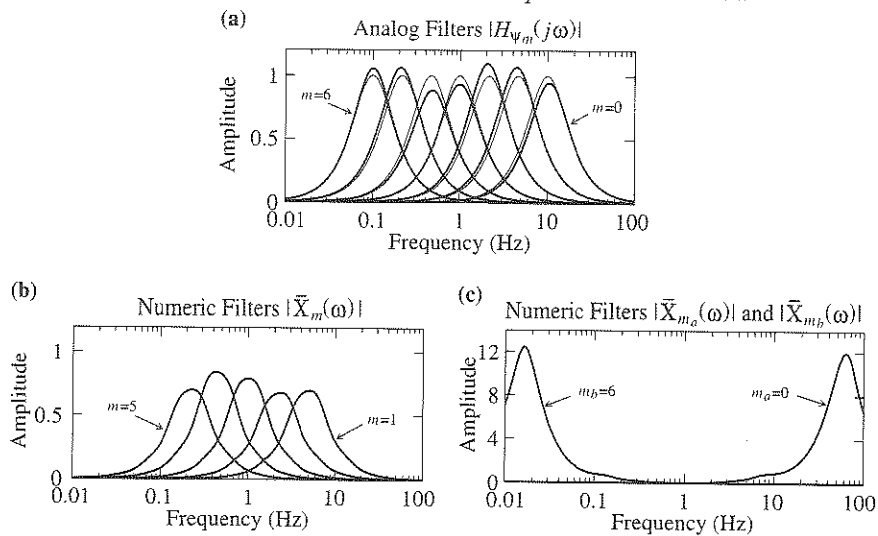


Fig. 2. a) Spectrums of the exact (thick) analog filters $H_{\psi_m}(j\omega)$, and with simulated linear variations (bold). b) Spectrums of the numerical filters $\bar{\mathbf{X}}_m(\omega)$ compensating linear variations. c) Spectrums of the numerical lateral filters, $\bar{\mathbf{X}}_{m_a}(\omega)$ and $\bar{\mathbf{X}}_{m_b}(\omega)$, compensating linear variations and band-pass behavior.

6 Conclusions

A mixed analog-digital approach to implement the WT has been explained, including a numerical compensation of the variations on the nominal values of the analog devices, as well as a method to numerically compensate the band-pass effects of the system due to the finite number of scales.

A simulated example has been presented, where the analysis capabilities of the analog direct WT, and the reconstruction virtues of the numerical inverse WT could be graphically appreciated.

The proposed methodology has been developed at the level of the linear systems theory, then, it can be applicable at any frequency, with the only limitations of the analog-to-digital conversion and the numerical processing rates.

Acknowledgments

 ${\rm M.\,A.\,Gurrola\,thanks\,Mexican\,Council}$ for Science and Technology (CONACYT) for his Doctoral Scholarship.

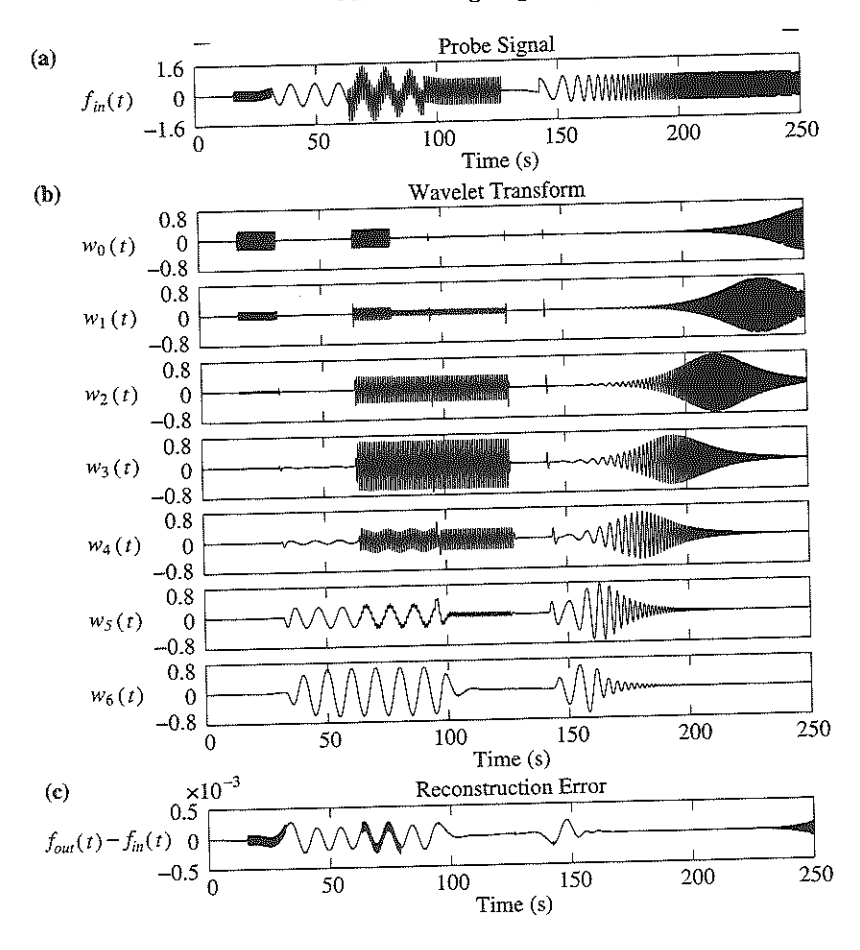


Fig. 3. a) Probe signal $f_{in}(t)$ including a chirp signal and oscillations of 0.1, 1.0 and 10 Hz. b) Wavelet transform $w_m(t)$. c) Error of reconstruction $f_{out}(t) - f_{in}(t)$.

References

- Addison, P.S.: The Illustrated Wavelet Transform Handbook: Applications in Science, Engineering, Medicine and Finance. Institute of Physics Publishing, Bristol (2002)
- Unser, M., Aldroubi, A.: A review of wavelets in biomedical applications. In: Proceedings of the IEEE. Volume 84. (1996) 626–638
- 3. Sadowsky, J.: Investigation of signal characteristics using the continuous wavelet transform. Johns Hopkins APL Thechnical Digest 17 (1996) 258–269
- Lin, J., et al.: Analog vlsi implementations of auditory wavelet transforms using switched-capacitor circuits. IEEE Trans. Circuits Syst. I 41 (1994) 572–583
- Ortiz-Balbuena, L., et al.: Wavelets generation using laguerre analog adaptive filter. In: IEEE ISCAS'96. Volume 1. (1996) 325–328

Table 2. Maximum difference, $f_{out}(t) - f_{in}(t)$, as a function of the number n of extra scales considered in the lateral filters $\bar{X}_{m_a}(\omega)$ and $\bar{X}_{m_b}(\omega)$.

extra scales	max. error
n	
0	1.1×10^{-1}
1	5.9×10^{-3}
2	2.7×10^{-4}
3	1.3×10^{-5}
4	6.3×10^{-7}
5	2.9×10^{-8}

The maximum amplitude of $f_{in}(t)$ is 1.5

- Kamada, H., Aoshima, N.: Analog gabor transform filter with complex first order system. In: Proc. 36th SICE Annual Conference, International Session Papers. (1997) 925–930
- Chen, D., Harris, J.G.: An analog vlsi circuit implementing an orthogonal continuous wavelet transform. In: Proc. IEEE International Conference on Electronics, Circuits and Systems. Volume 2. (1998) 139–142
- 8. Haddad, S.A.P., et al.: Analog wavelet transform employing dynamic translinear circuits for cardiac signal characterization. In: Proc. IEEE International Symposium on Circuits and Systems. Volume 1. (2003) I-121 I-124
- 9. Gurrola-Navarro, M.A., Espinosa-Flores-Verdad, G.: Direct and inverse wavelet transform implemented usign continuous filters. In: Proc. IEEE 48th Midwest Symposium on Circuits and Systems. Volume 2. (2005) 1051–1054
- 10. Chui, C.K.: Wavelet Analysis and its Applications Volume 1: An Introduction To Wavelets. Harcourt Publishers Ltd, San Diego (1992)
- Mallat, S., Zhong, S.: Characterization of signals from multiscale edges. IEEE Trans. Pattern Anal. Machine Intell. 14 (1992) 710-732